Electron Measurement at RHIC

Y. Akiba[a] for the PHENIX Collaboration*

[a]KEK, High Energy Accelerator Research Organization, Tsukuba-shi, Ibaraki-ken 305-0801, Japan

Preliminary results of electron measurements at RHIC in Au+Au collisions at $\sqrt{s_{NN}}$ = 130 A GeV are presented. Inclusive electron spectra are measured from a few hundred MeV/c to 4 GeV/c in transverse momentum. Inclusive photon spectra are measured by conversion methods from a few hundred MeV/c to 3 GeV/c.

1. Introduction

One of the unique features of the PHENIX experiment is its ability to identify electrons in a wide momentum range, from a few hundred MeV/c to several GeV/c in p_t in the central rapidity region. With its two central spectrometer arms, PHENIX can measure electron pairs from the low mass region below the ρ mass to high mass region beyond the J/Ψ mass and up to Υ resonances.

Electron measurement is important in heavy ion physics since one can study almost the entire time development of the collision system, from the earliest parton collision stage to the latest hadron gas phase. One can probe each stage using different measurements with electrons which are roughly classified into the three categories described below.

The first category is measurement of "prompt" electrons, which are electrons that do not originate from conventional sources such as Dalitz decays (π^0 and η), di-electron decay of vector mesons (ρ, ω, and ϕ), or external conversion of photons. In the early 1970's, copious production of prompt electrons for p_t above 1 GeV/c at a level of signal $e/\pi \sim 2 \times 10^{-4}$ was observed in p + p collisions at the CERN ISR ($\sqrt{s} = 50$ - 63 GeV)[1–3]. A natural interpretation of the prompt electron is that it comes from the decay of charmed particles. At RHIC energies, the charm electron signal level is expected to be $e/\pi \sim 3$ - 4 $\times 10^{-4}$ in p+p collisions. If charm production scales as A^2, the signal level in Au+Au collision can be as high as 10^{-3}[4] since pion production is suppressed from A^2 scaling at RHIC, as it is reported in this conference[5–7]. Figure 1 shows a cocktail plot of the expected electron momentum distributions from various sources. In the low p_t region, electron from π^0 Dalitz decay dominate. Electrons from charm decay can become dominant at 1 to 2 GeV/c in p_t, depending on the level of charm production. For high p_t (above 3 or 4 GeV/c) the contributions from b-quark decay become dominant. The contribution from photon conversion in the beam pipe and detector material is not shown in the plot, but it is at about same level as the Dalitz contribution in the PHENIX. From

*For the full PHENIX Collaboration author list and acknowledgments, see the contribution by W. A. Zajc (K. Adcox*et al.*) in this volume.

the prompt electron measurements, one can determine charm production and thereby the gluon density at an early stage of the collision. The effect of gluon shadowing and the energy loss of fast-moving charm quarks in hot matter can be studied via the prompt electron spectrum. The charm measurement is also important to understand the nature of the J/Ψ suppression.

The second category is measurement of inclusive photons by an internal and external conversion method. The conversion method is complementary to photon measurement by electro-magnetic calorimeter, and it is particularly suited to measurements in the low p_t region, where the conversion method provides a clean measurement of identified photons from the collision vertex with better momentum resolution than can be achieved using calorimeteric techniques. A draw-back of this method is that the yield is suppressed by a factor of about 50 to 100, which is not a problem in the low p_t region where the cross section is large. The goal of the photon measurement is to find and measure thermal direct photons from the quark-gluon plasma.

The third category is the measurement of electron pairs in a roughly back-to-back configuration. This measurement provides much information, and is further divided into several topics by the effective mass region of e^+e^- pairs. At the high end of mass spectrum, the initial quark density can be studied from the Drell Yan process. The deconfinement transition is studied by the J/Ψ suppression[8]. The mass region between the J/Ψ and the ϕ is a good window to search for thermal lepton pairs from the quark gluon plasma[9]. In the low mass region, medium modification of vector meson properties in hot hadronic matter before freeze-out can be studied.

The PHENIX experiment can perform all measurements listed above. In the following, we report preliminary results of electron measurements by PHENIX from the first year run of RHIC in the summer of 2000.

2. Inclusive electron measurement

The PHENIX detector and its particle identification capability is described elsewhere[10–12]. For the inclusive electron measurement, the West Arm spectrometer is used. The entire solid angle of the Drift Chamber (DC), the Pad Chamber 1 (PC1), the Ring Imaging Cherenkov detector (RICH), and the lower half of the Electromagnetic Calorimeter (EMCAL) in the West Arm were read-out during the year 2000 run.

The vertex position, measured by the Beam Beam Counter (BBC), is required to be within 20 cm from Z=0, resulting in about 1.5 million minimum bias Au+Au events. Charged particle tracks are reconstructed using the tracking detectors (DC and PC1), and their momentum are reconstructed by the DC. The track is then confirmed by an associated hit in the EMCAL within 2 σ of the projected track hit position. Electron identification is performed using the RICH and the EMCAL. The analysis is limited to $p_t < 4$ GeV/c where the track momentum is well measured by the DC and a pion does not produce Cerenkov light in the RICH. It is required that at least 3 PMT hits in the RICH are associated with a track. In addition, a cut is applied to a quality factor calculated from the track projection point and the position of the associated RICH PMT hits. Although a hadron does not produce a signal in the RICH, it can be mis-identified as an electron by a random association with un-related hit PMTs in the RICH. This

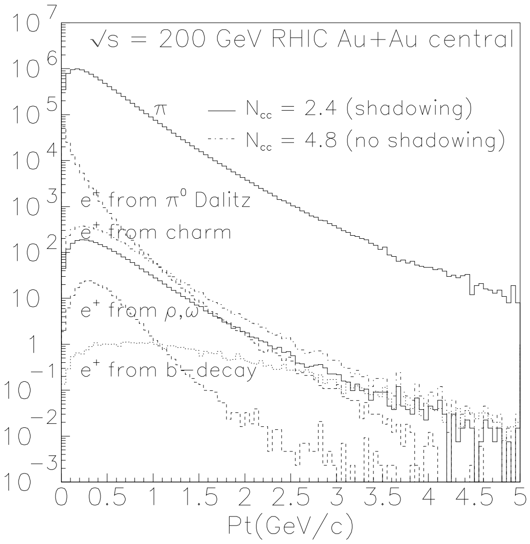

Figure 1. Electron spectrum expected at RHIC energies. Contributions from several electron sources are shown. See text for details.

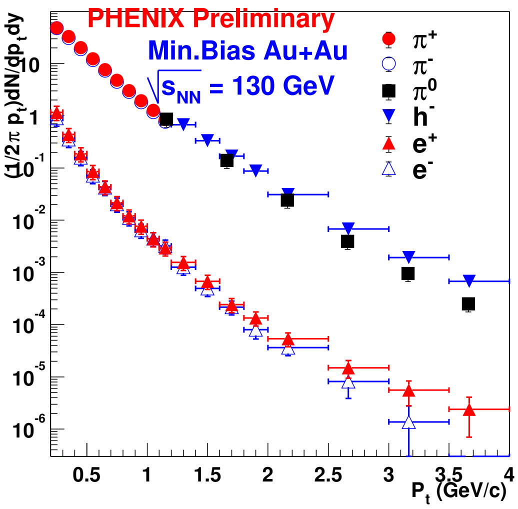

Figure 2. Inclusive transverse momentum distribution of e^+, e^-, π^+, π^-, π^0, and negative un-identified particles in Au+Au minimum bias collisions measured in the PHENIX West Arm spectrometer.

random mis-identification probability is less than 1 % in Au+Au minimum bias events. The hadron background is further reduced by requiring that the energy of the track, measured by the EMCAL, is more than 80 % of the momentum. The energy-momentum matching cut also removes background electrons from the photon conversion in the air far from the collision vertex. The conversion background is significant for $p_t > 1$ GeV/c before the energy-momentum cut is applied. The remaining background is produced when a hadron with a large energy deposition in the EMCAL is randomly associated with hits in the RICH. This random background is estimated by flipping the tracks with respect to Z=0 plane and then by applying the same electron ID cuts on the flipped track. The estimated random background is then subtracted from the data.

Figure 2 shows the inclusive spectra of e^+ and e^- in minimum bias Au+Au collisions. The spectra are corrected for the tracking efficiency, acceptance, and the electron identification efficiency. The electron spectra are measured up to 4 GeV/c, where the statistics run out. In the same plot, momentum spectra of π^+, π^-, and un-identified negative particles within the same acceptance are also plotted for comparison. In this analysis, the charged pions are identified using the time-of-flight measurement in the EMCAL up to 1.2 GeV/c in p_t. The neutral pion spectrum, measured in the same West Arm EMCAL, is also shown in the plot. Systematic uncertainties ($\sim \pm 30\%$) in the pion, negative hadron, and electron spectra are not shown in the figure. The electron spectra are two orders of magnitude below the pion spectra at low p_t, and they are three orders of magnitude below at high p_t.

The electron spectra include backgrounds such as Dalitz decays and photon conversions. A major part of those "trivial" background electrons is due to the neutral pions; it originates directly from π^0 Dalitz decay or indirectly from external conversion of photons from $\pi^0 \to \gamma\gamma$ decay. Therefore, the amount of the background can be determined from the pion spectrum measured in the same acceptance. The analysis is in progress to search for prompt electron component in the electron spectrum.

3. Inclusive Photon Measurement

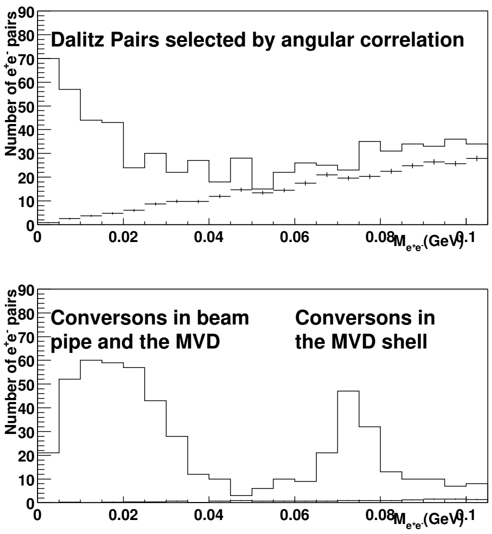

Figure 3. Low mass e^+e^- pairs from Au+Au collisions measured in the PHENIX. The top panel shows the pairs from $R \sim 0$ and the bottom panel shows the conversion pairs from $R > 0$. The crosses in each panel shows the combinatorial background estimated by an event mixing method. See the text for further explanation.

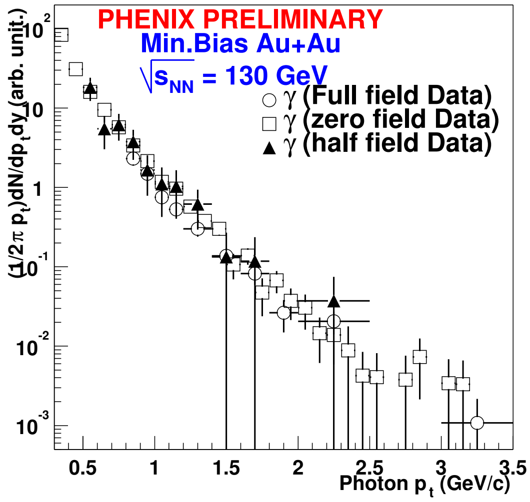

Figure 4. Photon spectra in Au+Au collisions at RHIC measured using the conversion methods. Results from three different analyses in full magnetic field, half field, and zero field data are shown.

Inclusive photons are measured by their conversion to a low mass e^+e^- pairs. Figure 3 shows the effective mass distributions of e^+e^- pairs detected in the West Arm. In order to increase the acceptance of the pair, the requirement for electron identification was relaxed, and only one of the e^+ or e^- tracks was required to hit the EMCAL. Even with this loose electron identification, clear enhancements due to Dalitz decay and external conversions are seen in the low mass region. There are structures in the enhancement; a broad peak at $M_{ee} = 0$ and another peak at $M_{ee} \sim 70$ MeV. The former is a mixture of the Dalitz decays and the conversions in the beam pipe and the MVD Si detector. The latter is the conversions in a thin outer enclosure of the MVD located at radius $R = 29$ cm from the beam line. Since the reconstruction assumes that all tracks come from the event vertex at $R = 0$, the reconstructed effective mass of a conversion e^+e^- pair from $R \neq 0$ is displaced from its real value. The displacement is roughly proportional to R. In addition, a conversion pair also acquires an apparent angular orientation such that the plane formed by e^+ and e^- at the assumed track origin ($R = 0$) is perpendicular to the magnetic field, which is parallel to the beam. This apparent angular orientation can be used to separate the Dalitz decays and the conversions.

The top panel of figure 3 shows the Dalitz pair candidates selected by the angular orientation, and the bottom panel shows the conversion candidates. The mass distribution of conversion pairs shows two peaks. The lower peak, at $M_{ee} \sim 10$ MeV, is from the beam pipe and the MVD Si detector. The higher peak is from the MVD outer shell. There is little combinatorial background in the conversion samples.

Figure 4 shows the inclusive photon p_t distribution obtained from the conversion analysis. It also shows photon distribution obtained using two additional conversion analyses from zero-field runs and half-field runs. In the zero-field run analysis, a conversion pair is identified by the matching of a cluster of hit PMTs in the RICH and a reconstructed cluster in the EMCAL, and the energy of the pair is measured by the EMCAL. All three photon distributions are corrected for acceptance along with the conversion probability in the known material within the acceptance. The spectra shows an exponential shape from a few hundred MeV/c to 3 GeV/c. The three analyses agree with one another within errors. Analysis is in progress to search for excess photons not explained by conventional hadronic sources such as π^0 and η decays.

4. Summary and Outlook

Figure 5 shows a preliminary effective mass distribution of electron pairs from the year 2000 data. In this analysis, two central arms of the PHENIX were used. Since calibration of the East Arm EMCAL was not completed, energy-momentum matching was not required for electron identification in the East Arm. This means that the background level in this mass spectrum is significantly higher. In the majority of the mass region, the mass distribution is consistent with the combinatorial background estimated using an event mixing method, as shown in the figure. A small deviation in the low mass region is mainly caused by the photon conversions. The mass spectrum extends to the J/Ψ region, where we do observe a few events. However, the statistics in the present data are too small to measure the J/Ψ, although the data show that the background level is already sufficiently low for a successful J/Ψ measurement.

In the coming run in 2001, PHENIX will accumulate a data set about three orders of magnitude larger than the present data set. The pair acceptance will be about a factor of 4 larger than the year 2000 run configuration since all detectors in the two central arms will be read-out. We expect to observe several thousand $J/\Psi \rightarrow e^+e^-$ and $\phi \rightarrow e^+e^-$ events from the coming run.

In summary, the PHENIX experiment measured e^+ and e^- from Au+Au collisions at $\sqrt{s_{NN}} = 130$ GeV. Inclusive electron spectra and inclusive photon spectra are obtained

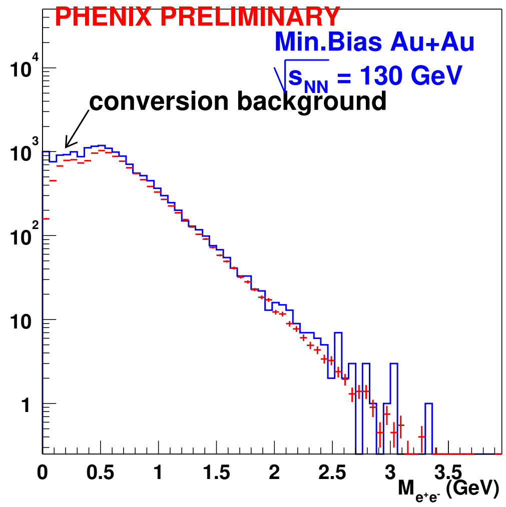

Figure 5. High mass e+e- pairs measured in the PHENIX.

from this measurement. Analysis is in progress to search for a prompt electron signal from charm decay and thermal direct photons. In the coming run, we will measure prompt electrons, inclusive photons, and high mass electron pairs with much higher statistics and with a much improved PHENIX detector.

REFERENCES

1. F.W. Büsser *et al.*,Nucl. Phys. B113 (1976) 189.
2. M. Basile *et al.*, Nouvo Cimento 65A (1981) 421.
3. P. Perez *et al.*, Phys. Lett. 112B (1982) 260.
4. Y. Akiba, *Proceedings. Physics with the Collider Detectors at RHIC and the LHC,* eds.: J. Thomas and T. Hallman, 1995, UCRL-ID-121571.
5. G. David for the PHENIX Collaboration, these proceedings.
6. F. Messer for the PHENIX Collaboration, these proceedings.
7. J. Dunlop for the STAR Collaboration, these proceedings.
8. T. Matsui and H. Satz, Phys. Lett. B178 (1986) 416.
9. P. V. Ruuskanen, Nucl. Phys. A544 (1992) 169c.
10. PHENIX Conceptual Design Report, BNL 1993 (unpublished).
11. D. P. Morrison for the PHENIX collaboration, Nucl. Phys. A638 (1998) 565c.
12. H. Hamagaki for the PHENIX Collaboration, these proceedings.